GEOPHYSICAL RESEARCH LETTERS, VOL. 37, L06311, doi:10.1029/2010GL042586, 2010

Very broadband analysis of a swarm of very low frequency earthquakes and tremors beneath Kii Peninsula, SW Japan

Akiko Takeo,[1] Koki Idehara,[1] Ryohei Iritani,[1] Takashi Tonegawa,[1] Yutaka Nagaoka,[1] Kiwamu Nishida,[1] Hitoshi Kawakatsu,[1] Satoru Tanaka,[2] Koji Miyakawa,[1] Takashi Iidaka,[1] Masayuki Obayashi,[2] Hiroshi Tsuruoka,[1] Katsuhiko Shiomi,[3] and Kazushige Obara[3]

Received 18 January 2010; revised 22 February 2010; accepted 25 February 2010; published 31 March 2010.

[1] We have conducted a temporal broadband seismic observation in Kii Peninsula, southwest Japan, and detected a swarm of 110 very low frequency earthquakes (VLFs) and deep low frequency tremors. During three days of the swarm activity, VLFs and tremors occur concurrently in two localized regions separated by ~10 km. Stacking analyses are also employed to detect VLF signals of a period longer than 50 s, whose focal mechanisms are determined for the first time from data and shown to be consistent with the subducting plate motion. Evaluation of the VLF seismic moment implies that a substantial portion of the SSE seismic moment is released as a VLF swarm.
Citation: Takeo, A., et al. (2010), Very broadband analysis of a swarm of very low frequency earthquakes and tremors beneath Kii Peninsula, SW Japan, *Geophys. Res. Lett.*, *37*, L06311, doi:10.1029/2010GL042586.

1. Introduction

[2] A new class of earthquakes called slow earthquakes have been discovered in worldwide subduction zones. They are classified into three types by observable frequency bands: (i) Slow slip event (SSE) is a transient slip at a plate interface observed by GPSs, borehole strainmeters and borehole tiltmeters, and lasts several days to months [*Dragert et al.*, 2001; *Obara et al.*, 2004]. (ii) Non-volcanic deep low frequency tremor (tremor hereafter) is a long continuous signal of 1–10 Hz [*Obara*, 2002] coming from a plate interface [*Shelly et al.*, 2006]. Its swarm often coincides with SSE in Cascadia [*Rogers and Dragert*, 2003], southwest Japan [*Obara et al.*, 2004], etc. (iii) Deep very low frequency earthquake (VLF) is a signal of 20–200 s observed so far in southwest Japan by broadband seismometers and tiltmeters [*Ito et al.*, 2007; *Ide et al.*, 2008]. These slow earthquakes occur at down-dip side of seismogenic region on plate interface. For example in southwest Japan, they occur on the subducting Philippine Sea Plate interface at a depth of 35–45 km [*Obara*, 2009]. Therefore slow earthquakes are very important for understanding subduction processes.

[3] In particular, VLFs may be a key that bridges tremors and SSEs, but our knowledge is still limited. The fault plane solution is consistent with the subducting plate motion, they migrate together with tremors [*Ito et al.*, 2007], and moment rate functions are proportional to the tremor energy [*Ide et al.*, 2008]. To investigate VLFs further, we conducted the Nankaido NEtwork Campaign for Episodic-Slow-Slip Array observation (Nankaido-NECESSArray, hereafter N2-Array) in Nankaido region, southwest Japan.

2. Observation and Data

[4] We installed three-component broadband seismometers, CMG-3T in small buildings at five observation sites of Earthquake Research Institute, the University of Tokyo, and nine Hi-net observation sites of National Research Institute for Earth Science and Disaster Prevention (NIED) in Kii Peninsula (Figure 1a). The observation period is from October 2008 to March 2009, and it is the first dense broadband observation conducted in this region. As tremor swarms occur nearly every three months there, we recorded a swarm of VLFs and tremors from 10 to 12 November 2008. Figure 2 shows velocity waveforms of VLFs and tremors in three different frequency bands, for which detailed analyses will be given below. We also use data of permanent observation networks, Hi-net velocity seismometer, Hi-net tiltmeter and F-net broadband seismometer operated by NIED [*Okada et al.*, 2004].

3. Tremors

[5] Tremor sources are located by the envelope cross correlation method following *Suda et al.* [2009]. Vertical velocity waveforms are first filtered by a 5-th order Butterworth filter with a 2–8 Hz pass-band, converted to envelope waveforms using the Hilbert transformation, and smoothed by a low-pass filter of cutoff frequency at 0.5 Hz. A cross-correlation function between every pair of envelopes is then calculated with 60 s-long time window at every 30 s, and a lag time of an i-th pair of waveforms, Δt_i which gives a maximum cross-correlation coefficient C_i is estimated. To locate hypocenters, we use those pairs with C_i greater than 0.5, and a weighted root mean square of residual

$$\mathrm{RMS} = \sqrt{\frac{\sum_i C_i^2 \left(\Delta t_i - \Delta t_i^{\mathrm{pred}}\right)^2}{\sum_i C_i^2}}$$

[1]Earthquake Research Institute, University of Tokyo, Tokyo, Japan.
[2]Institute For Research on Earth Evolution, Japan Agency for Marine-Earth Science and Technology, Yokosuka, Japan.
[3]National Research Institute for Earth Science and Disaster Prevention, Tsukuba, Japan.

0094-8276/10/2010GL042586

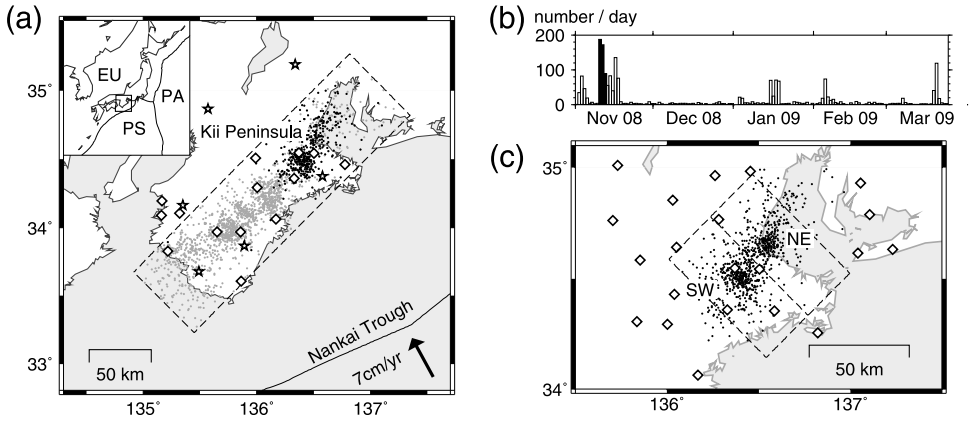

Figure 1. (a) Tremor epicenters during the N2-Array observation period (gray dots), and those during the stationary swarm activity in 10–12 November 2008 (black dots) located using vertical components of N2-Array (diamonds) and F-net (stars) stations. Dashed lines show the area searched for tremors. (b) The number of tremor detections per day. (c) Tremor epicenters during the stationary swarm activity (dots) located using Hi-net stations (open diamonds). Dashed lines separate two source regions, NE and SW.

is minimized by a grid search; the theoretical travel time difference Δt_i^{pred} is calculated using the S-wave velocity structure of JMA2001 [*Ueno et al.*, 2002], which Japan Meteorological Agency uses in their routine analysis. The grid intervals are 0.0025 degree in horizontal and 2 km in depth. We limit the search area as shown in Figure 1a considering the network coverage and previously known tremor activities. Criteria for a tremor detection are (i) the number of used pairs exceeds 10, (ii) the RMS is lower than 3 s, and (iii) the station average of maximum STA/LTA in the time window is lower than 3, where STA/LTA is the ratio of short time (2 s) average to long time (30 s) average that takes large values for impulsive signals from ordinary earthquakes.

[6] Figure 1a shows epicenters determined using 14 N2-Array and 6 F-net stations. The epicenter distribution is similar to that previously reported by *Obara* [2009], i.e., tremors are located at the down-dip side of the seismogenic zone. From the histogram of the tremor activity in Figure 1b, five swarm activities can be recognized for the entire study region. The most active swarm starts on 10 November 2008 at the east side of Kii Peninsula and lasts for three days. After this stationary activity, the swarm migrates toward southwest direction at velocity of 6–8 km/day.

[7] Tremor sources during the stationary swarm activity in 10–12 November 2008 are further determined using data of 21 Hi-net borehole stations, which provide lower noise data, and cover the source area much denser than N2-Array and F-net. Their epicenter distribution in Figure 1c shows that the sources are concentrated in two regions, southwest (SW) and northeast (NE), separated from each other by at least 10 km. By bootstrap of 100 samples, epicenter errors are estimated to be within 10 km in both longitude and latitude directions. The located depths range in 20–40 km with a peak at 32 km and errors are mostly within 10 km.

4. VLFs (20–50 s)

[8] We determine the centroid origin time, location and moment tensor of VLFs using the GRiD MT method [*Tsuruoka et al.*, 2009] with vertical components from two N2-Array stations, three components from a F-net station, and horizontal components from eight Hi-net tiltmeters. Synthetic seismograms are calculated using a program developed by *Takeo* [1987]. The velocity structure is the same as that of the F-net moment tensor inversion operated in Japan [*Kubo et al.*, 2002]. We apply a 20–50 mHz 8-th order Butterworth filter to observed velocity waveforms

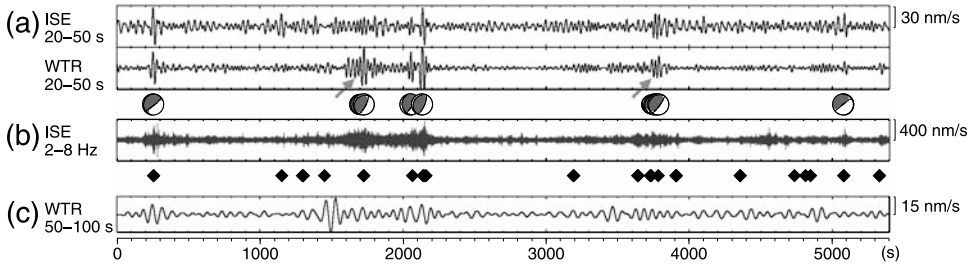

Figure 2. Observed vertical velocity waveforms during 90 minutes from 11 November 2008, 6:59 (GMT) at a N2-Array station ISE and a F-net station WTR (Figure 3a). (a) VLF waveforms and determined moment tensor solutions in lower-hemisphere projection. Arrows mark continuous signals of 100–300 s. (b) Tremor waveform and peak times used as the reference time for stacking (diamonds). (c) VLF waveform with a period longer than 50 s. Individual waveforms of other stations are too noisy to detect VLF signals in this frequency band.

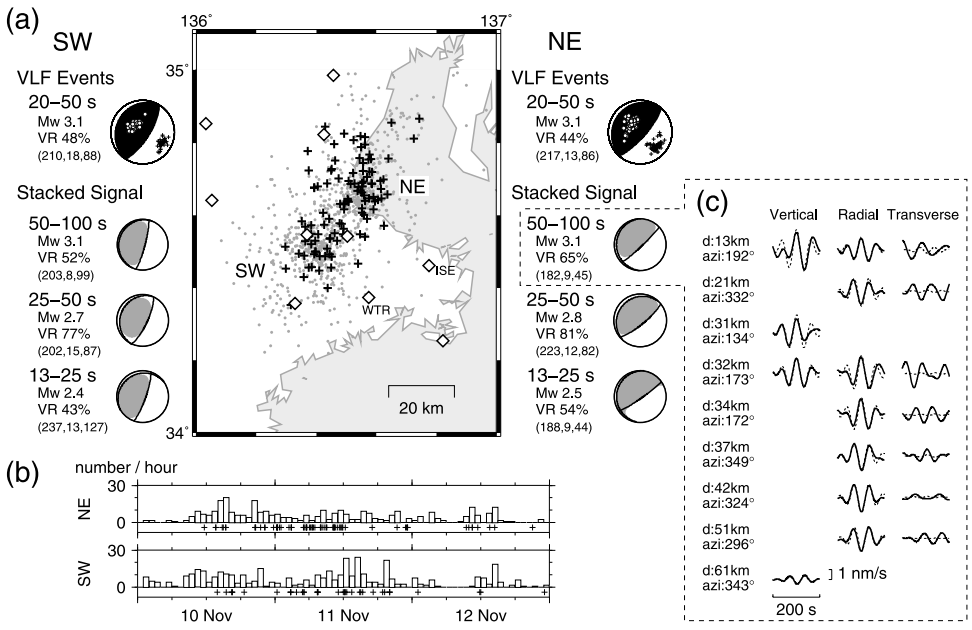

Figure 3. VLFs and tremors during the swarm period, 10–12 November 2008. (a)VLF epicenters (crosses) detected by using data of broadband stations (diamonds). Gray dots show tremor epicenters. A beach ball at the top of each side shows the average source mechanism of VLF events for each region; T-axes (circles) and P-axes (crosses) of individual solutions are also shown. Other beach balls are the mechanisms corresponding to the stacked waveforms. The bottom caption for each beach ball indicate (strike, dip, rake) of the fault-plane solution. (b) The number of tremors used for stacking in each source region is given in a histogram for every one hour. Crosses at the bottom indicate times of VLF occurrence. (c) An example set of stack averaged velocity waveforms (solid lines) and synthetics (dashed lines) with a 200 s time-window. The corresponding solution (NE, 50–100 s stacked signals in (a)) is surrounded by a broken line. Captions at the left-side indicate epicenter distance and azimuth.

$f_i^{\mathrm{obs}}(t)$ and synthetics $f_i^{\mathrm{syn}}(t)$. To obtain moment tensor solutions, we conduct a grid-search by minimizing variance reduction

$$\mathrm{VR} = \left[1 - \frac{\sum_i \int \left\{f_i^{\mathrm{obs}}(t) - f_i^{\mathrm{syn}}(t)\right\}^2 dt}{\sum_i \int \left\{f_i^{\mathrm{obs}}(t)\right\}^2 dt}\right] \times 100\ \%$$

with 120 s time-window. The grid intervals are 0.05 degree in horizontal, 5 km in depth, and 1 s in time. Detection criteria of VLF are (i) VR is greater than 30%, and (ii) bootstrap estimated epicenter error is lower than 15 km. Since we frequently detect a mechanism and its reversed one from continuous oscillation of VLF signals and isolated signals always result in reverse fault solutions, we manually eliminate normal fault solutions. For each detected VLF, we use bootstrap averaged epicenter and moment tensor as the final solution. We also take the shallowly dipping nodal plane of the best-double-couple solution as the fault-plane.

[9] In total, 110 VLF events are detected during the stationary activity of tremors in 10–12 November 2008. The number of detection is one order of magnitude larger than that for previously reported VLF activities. Their moment magnitudes, 2.9–3.3, are smaller than Mw 3.1–3.8 in past studies [*Ito et al.*, 2007, 2009]. These results originate from the occurrence of an unusually high VLF swarm activity, and a happy coincidence that the N2-Array stations are deployed right above the source regions. If we use displacement waveforms (instead of velocities) and a higher threshold of VR following past studies, the number of event detection is reduced less than a half but is still significantly larger than those of previously reported activities. Figure 3a shows VLF epicenters. We can recognize two active regions similar to those of tremors. The estimated source depth distribution shows a peak at 35 km and the errors are about 5–10 km. From waveforms, all VLF events seem to occur with tremors, but we can detect only 68 VLF-associated tremors with our current tremor detection criteria. The relative distance between a VLF and a tremor that occur in the same time window is less than 15 km for 62 events among those 68, suggesting that they occur in the same region. It should be noted that *Maeda and Obara* [2009] also revealed tremor coincident occurrence with 17 VLFs in Shikoku, southwest Japan.

5. Longer-Period (>50 s) VLFs

[10] Although the presence of long-period signals greater than 50 s is reported by *Ide et al.* [2008], their source mechanisms have not been determined from observed data. The detection of many VLFs in this swarm activity encourages us to determine the mechanism in such a long period. We assume that long-period signals exist at the peak time of tremor, and stack long-period waveforms to detect the signal. For all tremors located by Hi-net data, envelope waveforms are aligned by the theoretical travel times from the source, and stacked. The peak time of stacked envelopes is used as the reference time to stack long-period data. When two consecutive tremor time-windows show similar peak times, we take the mean value. Time-windows that

show arrivals of teleseismic surface waves are also eliminated before stacking. The resultant total number of reference event peaks are 369 for the NE region, and 437 for the SW region. We then align long-period waveforms filtered with the period range of 50–100 s at the reference times, and average them for each region. For further analysis, we select waveform data whose (i) peak value exceeds twice the standard error, or (ii) in case of a horizontal component, one of two horizontal components satisfies (i); as a result, 18 components from 9 stations and 20 components from 10 stations are selected for NE and SW regions, respectively. We finally determine the epicenter and zero trace moment tensor with 200 s time-window using the same method as that of VLF detection, except for the source depth fixed at 35 km.

[11] Figure 3c shows an example of waveform fit. Figure 3a shows the bootstrap averaged mechanisms. Estimated errors for epicenters are 5–10 km. Within the margin of error, mechanisms are consistent with the subducting plate motion, and the epicenters are located in the same region as those of tremors used to measure reference times. The destructive interference effect from phase misalignment seems minor because the magnitude, Mw 3.1, is comparable with those of individual VLF events, Mw 2.9–3.3, estimated in the previous section.

[12] Using the same selected waveforms, period ranges of 25–50 s and 13–25 s are also analyzed with 120 s time-window. Obtained mechanisms in Figure 3a are similar to those of VLF events, and suggest that the stacking method employed here that uses a tremor envelope peak as a reference is reasonable. We have also tried other references, such as the 20–50 mHz VLF origin time, but this method works best. Smaller magnitudes in higher frequencies may indicate an destructive interference effect from misaligned phases. We can not determine the mechanism in lower and higher frequency ranges because of the low signal-to-noise ratio.

6. Discussion

[13] A SSE of Mw 6.3 is detected by *Geological Survey of Japan* [2008] using strain changes during the VLF swarm period in 10–12 November 2008. *National Research Institute for Earth Science and Disaster Prevention* [2009] also detected a SSE of Mw 6.2 using tilt changes in 10–14 November 2008. In the SSE fault area, VLFs coincided with tremors. One interpretation of these phenomena is that VLFs and tremors occur at different patches on the SSE fault area [*Ito et al.*, 2007]. Another interpretation is that tremor and VLF are the same phenomenon which we observe in different frequencies [*Ide*, 2008].

[14] The VLF contribution to SSE moment releases is estimated to be 0.1% by *Ito et al.* [2009], but they included only detectable VLF signals. We account for almost all signals by stacking analysis, and can estimate the contribution more precisely. Using the magnitude Mw 3.1 of stack averaged waveforms in the period of 50–100 s and the number of stacking, the total VLF moment release in the frequency range becomes equivalent to Mw 5.0, which is 1–2% of the SSE seismic moment. This value could be still largely underestimated if the VLF source duration is comparable or longer than the period range of analysis. For example, *Ide et al.* [2008] analyzed VLFs of duration up to 200 s and showed that the estimated seismic moment could be over 5 times larger than that estimated in the conventional frequency band of VLF analyses. If continuous VLF and tremor signals (Figure 2) reflect such a long source duration, a substantial amount (say up to 5–10%) of SSE seismic moment is released as VLFs. It should be noted that *Matsuzawa et al.* [2009] estimated VLF durations in Shikoku to be 12–18 s.

[15] The relative magnitude of VLF and tremor is another topic of interest. We observe a correlation between VLF moment and tremor energy rate with a correlation coefficient of 0.61, where we estimate tremor energy rate from the peak of envelope waveforms. For detailed comparison, however, we must obtain VLF source time functions such as *Ide et al.* [2008] by the observation of long-period VLFs in many stations.

[16] **Acknowledgments.** Nankaido-NECESSArray was conducted as a part of "Frontier observation project" (2007-B-01) supported by the Earthquake Research Institute cooperative research program, and the data will be available from the OHP data management center of ERI. A part of this research was conducted as the undergraduate (A. T. and Y. N.) exercise course of the University of Tokyo (SchoolYear2008). We thank Minoru Takeo for providing a software to calculate synthetics, Mare Yamamoto and Takanori Matsuzawa for comments on the manuscript. Two reviewers, Naoki Suda and Justin Rubinstein, also provided helpful suggestions. We used the Generic Mapping Tools [*Wessel and Smith*, 1998] to draw figures.

References

Dragert, H., K. Wang, and T. S. James (2001), A silent slip event on the deeper Cascadia subduction interface, *Science*, *292*, 1525–1528.

Geological Survey of Japan (2008), Strain Changes associated with the SSE in Kii Peninsula (in Japanese), *Rep. 81 8-3*, pp. 502–521, Coord. Comm. Earthquake Predict., Ibaraki, Japan.

Ide, S. (2008), A Brownian walk model for slow earthquakes, *Geophys. Res. Lett.*, *35*, L17301, doi:10.1029/2008GL034821.

Ide, S., K. Imanishi, Y. Yoshida, G. C. Beroza, and D. R. Shelly (2008), Bridging the gap between seismically and geodetically detected slow earthquakes, *Geophys. Res. Lett.*, *35*, L10305, doi:10.1029/2008GL034014.

Ito, Y., K. Obara, K. Shiomi, S. Sekine, and H. Hirose (2007), Slow earthquakes coincident with episodic tremors and slow slip events, *Science*, *315*, 503–506.

Ito, Y., K. Obara, T. Matsuzawa, and T. Maeda (2009), Very low frequency earthquakes related to small asperities on the plate boundary interface at the locked to aseismic transition, *J. Geophys. Res.*, *114*, B00A13, doi:10.1029/2008JB006036.

Kubo, A., E. Fukuyama, H. Kawai, K. Nonomura (2002), NIED seismic moment tensor catalogue for regional earthquakes around Japan: Quality test and application, *Tectonophysics*, *356*, 23–48.

Maeda, T., and K. Obara (2009), Spatiotemporal distribution of seismic energy radiation from low-frequency tremor in western Shikoku, Japan, *J. Geophys. Res.*, *114*, B00A09, doi:10.1029/2008JB006043.

Matsuzawa, T., K. Obara, and T. Maeda (2009), Source duration of deep very low frequency earthquakes in western Shikoku, Japan, *J. Geophys. Res.*, *114*, B00A11, doi:10.1029/2008JB006044.

National Research Institute for Earth Science and Disaster Prevention (2009), Short-term slow slip event with non-volcanic tremors in southwest Japan (November, 2008–April, 2009)(in Japanese), *Rep. 82 9-2*, pp. 392–397, Coord. Comm. Earthquake Predict., Ibaraki, Japan.

Obara, K. (2002), Nonvolcanic deep tremor associated with subduction in southwest Japan, *Science*, *296*, 1679–1681.

Obara, K. (2009), Inhomogeneous distribution of deep slow earthquake activity along the strike of the subducting Philippine Sea Plate, *Gondwana Res.*, *16*, 512–526, doi:10.1016/j.gr.2009.04.011.

Obara, K., H. Hirose, F. Yamamizu, and K. Kasahara (2004), Episodic slow slip events accompanied by non-volcanic tremors in southwest Japan subduction zone, *Geophys. Res. Lett.*, *31*, L23602, doi:10.1029/2004GL020848.

Okada, Y., K. Kasahara, S. Hori, K. Obara, S. Sekiguchi, H. Fujiwara, and A. Yamamoto (2004), Recent progress of seismic observation networks in Japan Hi-net, F-net, K-NET and KiK-net, *Earth Planets Space*, *56*, xv–xxviii.

Rogers, G., and G. Dragert (2003), Episodic tremor and slip on the Cascadia subduction zone: The chatter of silent slip, *Science*, *300*, 1942–1943.

Shelly, D. R., G. C. Beroza, S. Ide, and S. Nakamura (2006), Low-frequency earthquakes in Shikoku, Japan, and their relationship to episodic tremor and slip, *Nature*, *442*, 188–191.

Suda, N., R. Nakata, and T. Kusumi (2009), An automatic monitoring system for nonvolcanic tremors in southwest Japan, *J. Geophys. Res.*, *114*, B00A10, doi:10.1029/2008JB006060.

Takeo, M. (1987), An inversion method to analyze the rupture processes of earthquakes using near-field seismograms, *Bull. Seism. Soc. Am.*, *77*, 490–513.

Tsuruoka, H., H. Kawakatsu, and T. Urabe (2009), GRiD MT (grid-based real-time determination of moment tensors) monitoring the long-period seismic wavefield, *Phys. Earth Planet. Inter.*, *175*, 8–16.

Ueno, H., S. Hatakeyama, T. Aketagawa, J. Funasaki, and N. Hamada (2002), Improvement of hypocenter determination procedures in the Japan Meteorological Agency (in Japanese), *Q. J. Seismol.*, *65*, 123–134.

Wessel, P., and W. H. F. Smith (1998), New, improved version of Generic Mapping Tools release, *Eos Trans. AGU*, *79*(47), 579, doi:10.1029/98EO00426.

K. Idehara, T. Iidaka, R. Iritani, H. Kawakatsu, K. Miyakawa, Y. Nagaoka, K. Nishida, A. Takeo, T. Tonegawa, and H. Tsuruoka, ERI, University of Tokyo, 1-1-1 Yayoi, Bunkyo-ku, Tokyo 113-0032, Japan. (akiko-t@eri.u-tokyo.ac.jp)

K. Obara and K. Shiomi, NIED, 3-1 Tenno-dai, Tsukuba, Ibaraki 305-0006, Japan.

M. Obayashi and S. Tanaka, IFREE, JAMSTEC, 2-15 Natsushima-Cho, Kanagawa 237-0061, Japan.